ChemPubSoc Europe

DOI: 10.1002/chem.201902113

CHEMISTRY A European Journal Full Paper

Glycan Remodeling

Switchable Enzymatic Accessibility for Precision Cell-Selective Surface Glycan Remodeling

Peiwen Zhang, Yiran Li, Xiaofei Yu, Huangxian Ju, and Lin Ding*[a]

Abstract: Precision cell-selective surface glycan remodeling is of vital importance for modulation of cell surface dynamics, tissue-specific imaging, and immunotherapy, but remains an unsolved challenge. Herein, we report a switchable enzymatic accessibility (SEA) strategy for highly specific editing of carbohydrate moieties of interest on the target cell surface. We demonstrate the blocking of enzyme in the inaccessible state with a metal-organic framework (MOF) cage and instantaneous switching to the accessible state through disassembly of MOF. We further show that this level of SEA regulation enables initial guided enzyme delivery to the target cell surface for subsequent cell-specific glycan remodeling, thus providing a temporally and spatially controlled tool for tuning the glycosylation architectures. Terminal galactose/*N*-acetylgalactosamine (Gal/GalNAc) remodeling and terminal sialic acid (Sia) desialylation have been precisely achieved on target cells even with other cell lines in close spatial proximity. The SEA protocol features a modular and generically adaptable design, a very short protocol duration (ca. 30 min or shorter), and a very high spatial resolving power (ability to differentiate immediately neighboring cell lines).

Introduction

Cell surfaces feature a sophisticated collection of molecular components for interacting with and responding to the external environment.[1] Among this mosaic repertoire of appendages, glycans represent the most complex, diverse group and serve as a critical handle for mediating cell recognition, cell communication, cell adhesion, and immune response.[2a] Glycosylation is a non-template-driven biosynthesis process that is inherently cell type- or cell population-dependent.[2b] For example, hypersialylation is a phenotypic signature displayed by tumor cells to evade immune surveillance.[3] The ability to target a specific type or population of cells for glycan remodeling is therefore essential for the full understanding and precise modulation of glycan functions,[4a] tissue-specific glycan imaging,[4b,c] and tumor immunotherapy.[5] Previous attempts at developing cell-selective glycan remodeling methods rely on either indirect internal metabolic pathway[6] or direct external enzymatic action.[5a] The internal metabolic approach allows the achievement of cell specificity as it operates via initial guided delivery of metabolic precursor to target cells for subsequent glycan remodeling, but can suffer from undesired whole-cell perturbation (on both intracellular and extracellular proteins), unintended glycosylation site, and lengthy protocol duration issues.[6] The documented external enzymatic approach is plagued by compromised cell specificity because the enzyme is catalytically active toward unavoidable glycan remodeling on non-targeted cell surface during its supposedly guided delivery to target cell surface.[5a] To address these issues, herein we report a switchable enzymatic accessibility (SEA) method for precision cell-selective surface glycan remodeling (Scheme 1).

SEA is a general, versatile designer platform for cell-selective surface structural remodeling, and exploits the combined use of an enzymatic accessibility-regulating caging probe component (metal-organic framework, or MOF) and a cell-targeting recognition probe component (aptamer). Briefly, a two-stage protocol is used: the first stage is the delivery of MOF-encapsulated, catalytically inaccessible enzyme to target cell surface via aptamer binding (the accessibility of enzyme is blocked by MOF and no glycan remodeling occurs at this stage; if the enzyme is not blocked and glycan remodeling occurs at this stage, non-targeted cells will be modified). The second stage is the local release of enzyme (switched to the catalytically accessible state) on the target cell surface via MOF disassembly (local release is possible due to slow diffusion rate for a macromolecular-sized species such as enzyme[7]) for glycan remodeling of only target cells. This contrasts with the direct addition of enzyme, which will cause non-discriminatory, non-cell-selective surface glycan remodeling. Liang et al. have pioneered the use of MOFs as protective coatings for biomacromolecules:[8] in one application, they demonstrate the individual coating of enzyme and enzyme substrate each with respective MOFs (the accessibility of both enzyme and enzyme substrate are blocked) as well as their subsequent release for enzymatic reaction;[8a] in another proof of utility, they exploit the enzymatic

[a] *P. Zhang, Y. Li, X. Yu, Prof. Dr. H. Ju, Prof. Dr. L. Ding*
State Key Laboratory of Analytical Chemistry for Life Science
School of Chemistry and Chemical Engineering
Nanjing University, Nanjing 210023 (P.R. China)
E-mail: dinglin@nju.edu.cn

Supporting information and the ORCID identification number(s) for the author(s) of this article can be found under: https://doi.org/10.1002/chem.201902113.

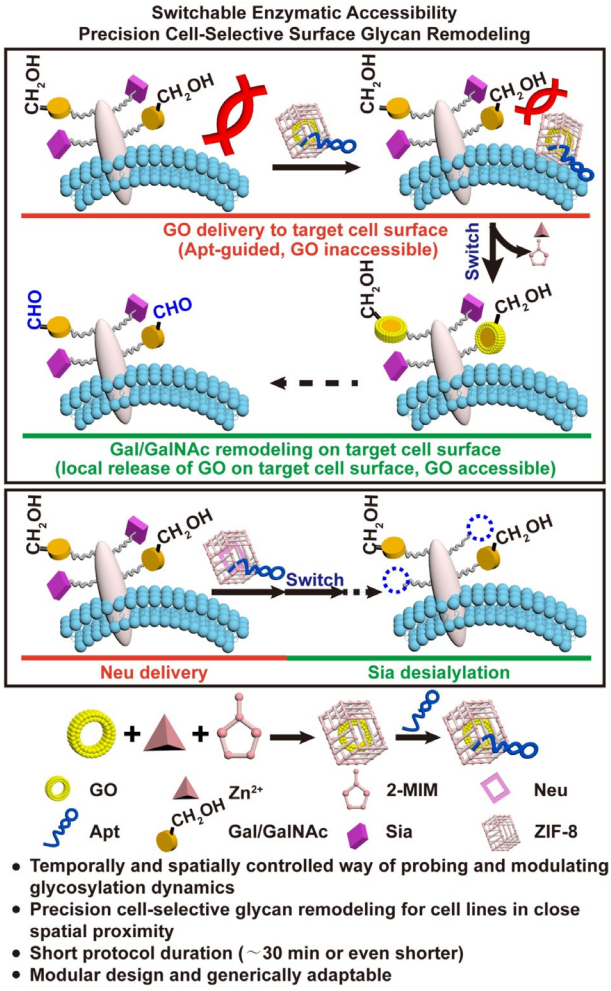

Scheme 1. Schematics of switchable enzymatic accessibility (SEA) strategy for precision cell-selective surface glycan remodeling.

accessibility under MOF coating to a freely diffusible small molecule substrate (lactose) to enable the survival of yeast cells in nutrient-deficient media.[8b] Herein we have introduced a fundamentally different concept, SEA: the encapsulation of enzyme alone with MOF will block its enzymatic accessibility to macromolecular-sized enzyme substrate (itself not blocked) and cell surface-confined, non-freely diffusible enzyme substrate (itself not blocked), and disassembly of MOF will enable the switching of enzyme to the accessible state for remodeling of substrate. As the natural target structure to be remodeled should in principle not be blocked, the SEA strategy essentially provides a general, spatially (cell-selective remodeling due to high effective local enzyme molarity[7]) and temporally (arbitrarily settable remodeling timing point) controlled way of accurate structural remodeling. Previous caging methods typically target the off-on switchability of intrinsic enzyme function (distortion or occupation of catalytic center through photo-caging or inhibitor), and the covalent or noncovalent interaction can lead to slow restoration kinetics and even partial loss of catalytic activity;[9] SEA explores extrinsic enzymatic accessibility as a control, and, with enzyme loosely detached from MOF and extremely fast disassembly kinetics for MOF,[8e] the enzymatic accessibility can be instantaneously switched on with the full retention of catalytic activity.[10]

Results and Discussion

For the initial proof-of-concept study, galactose (Gal) oxidase (GO), which is capable of remodeling the C6-hydroxy group of terminal Gal/*N*-acetylgalactosamine (GalNAc) to the corresponding aldehyde group,[11] and zeolitic imidazolate framework-8 (ZIF-8), a biocompatible size-tunable MOF that can be synthesized under mild conditions,[12] were selected as the enzyme and accessibility-regulating reagent, respectively. Terminal Gal/GalNAc was selected as the remodeling target for its important contribution to cellular physiological function and neoplastic process.[13] ZIF-8 was synthesized at room temperature (r.t.) as uniform 660 nm rhombic dodecahedral crystals starting from Zn^{2+} and 2-methylimidazole (2-MIM),[12a] as evidenced by scanning electron microscopy (SEM) (Figure S1A), transmission electron microscopy (TEM) (inset in Figure S1A), and powder X-ray diffraction (PXRD) studies (Figure S1C). The participation of GO in the ZIF-8 assembly process did not alter the crystal phase, morphology, or size (Figure S1B,C). GO was both caged inside ZIF-8 and trapped on the outside surface. To strictly block GO accessibility, the surface-trapped GO needed to be removed, which could be conveniently achieved with polyvinylpyrrolidone (PVP) through competitive binding.[12b] Consistent with this, direct bicinchoninic acid (BCA) protein assay showed a reduced GO content (65.4% retention) after PVP treatment. The GO@ZIF-8 obtained thereof, with GO in the exclusively caged state inside ZIF-8, exhibited a roughened surface (Figure 1 A), contrasting with the smooth outlook for iden-

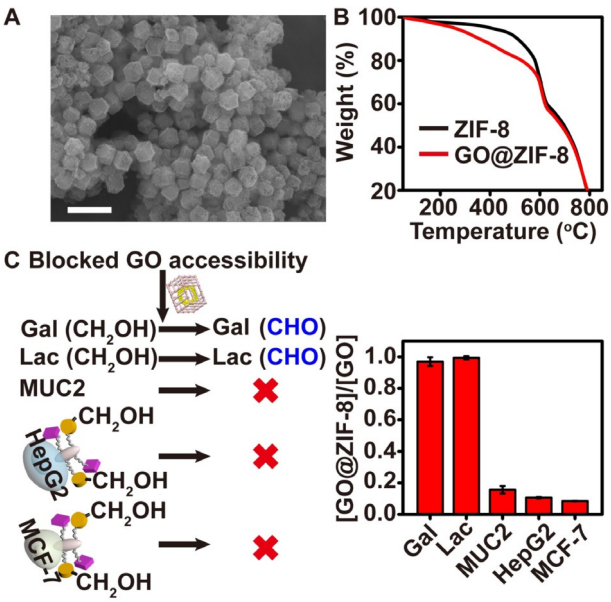

Figure 1. Blocking of GO accessibility to macromolecular-sized substrate and cell-surface structure with ZIF-8. A) SEM image of GO@ZIF-8 after PVP treatment. Scale bar: 1 μm. B) TGA traces of ZIF-8 and GO@ZIF-8 in air. C) Open GO accessibility to Gal and Lac but blocked GO accessibility to MUC2, HepG2 and MCF-7 cells as measured by the ratio of activity (symbolized as [ ]) between GO@ZIF-8 and GO.

tically treated pure ZIF-8 (Figure S2). The caging of GO in ZIF-8 was immediately apparent from infrared (IR) spectroscopy and thermal gravimetric analysis (TGA). A GO signature amide I band (1640 cm^{-1}) was observed for GO@ZIF-8 and absent for pure ZIF-8 (Figure S3). GO@ZIF-8 experienced an extra 7.9% weight loss from 200 °C to 510 °C as compared with pure ZIF-8, attributable to the decomposition of GO (Figure 1B). Given that GO contains a single copper center, quantification with inductively coupled plasma mass spectrometry (ICP-MS) for GO, pure ZIF-8, and GO@ZIF-8 allowed the estimate of weight percentage of GO in GO@ZIF-8 as approximately 5.6%. The weight percentage of GO in GO@ZIF-8 could also be calculated by comparing the zinc content of pure ZIF-8 and GO@ZIF-8, which amounted to approximately 5.4%. The embedding of GO inside ZIF-8 was also evident from the reduction in the apparent surface area and pore volume (Figure S4).

With GO@ZIF-8 successfully prepared, the catalytic activity of caged GO and accessibility-sifting property of ZIF-8 (with respect to substrate size dimension) were then evaluated. With a pore channel window of approximately 3.4 Å for ZIF-8, a small molecule substrate such as Gal or lactose (Lac) was expected to be capable of diffusing into the catalytic center of GO. Indeed, the GO activity in the caged state was fully preserved, exhibiting a virtually identical transforming efficiency compared with pristine GO, as assayed with the standard oxidase toolkit (Figures S1D and 1C). In contrast, for a macromolecular-sized substrate such as terminal Gal/GalNAc-presenting MUC2 protein, the accessibility of caged GO was substantially blocked, with its "apparent catalytic capacity" severely impaired (Figure 1C). The blocking of caged GO accessibility was also manifested on cell-surface-confined, non-freely diffusible structures, as GO@ZIF-8 showed minimal glycan remodeling capacity for HepG2 and MCF-7 cells (Figures 1C and S5).

With GO in the accessibility-blocking state demonstrated, the feasibility of switching to an accessible state was next assessed. Ethylenediaminetetraacetic acid (EDTA), a powerful chelating agent for Zn^{2+}, can override the coordination of 2-MIM and serve as an expeditious ZIF-8 disassembly effector.[8e] The released GO could function as a fully competent catalyst for Gal remodeling (Figure S1D), without any observable negative impact from EDTA or fragmented pieces of ZIF-8. Satisfactorily, the EDTA-liberated GO was indeed switched to the accessible state for cell surface glycan remodeling. The transformed terminal Gal/GalNAc, with aldehyde as the reaction handle, could be bioorthogonally labeled with fluorescein-5-thiosemicarbazide (TSC-FITC) and directly fluorescently imaged by confocal laser scanning microscopy (CLSM). The optimization of cell surface glycan remodeling setting was initially performed on pristine GO. For both HepG2 and MCF-7 cells, the fluorescence intensity of cell periphery reached a maximum at a GO concentration of approximately 0.05 mg mL^{-1} (Figures S6 and S7). This value could be taken as the optimum concentration of equally catalytically competent, caged GO in GO@ZIF-8 when unleashed for cell surface terminal Gal/GalNAc remodeling. The biocompatibility of EDTA was first evaluated in the context of cell surface glycan remodeling with GO. Neither the GO activity nor the physiological state of HepG2 and MCF-7 cells was compromised in EDTA (Figures S8). Further quantitative assay showed a high cell viability of HepG2 and MCF-7 cells in GO, ZIF-8, GO@ZIF-8, and EDTA (Figure S9). The execution of temporally controlled enzymatic accessibility switching on HepG2 cells, with EDTA as the timing point trigger, demonstrated the validity of the scheme (Figure 2A): the incubation of HepG2 cells in GO@ZIF-8 showed only background-level cell periphery fluorescence intensity, confirming blocked GO accessibility to cell surface. With the simultaneous participation of EDTA, the cell periphery fluorescence intensity rose to a level comparable to that achieved by pristine GO, suggesting high-efficiency switch-on of GO accessibility. The approach is designed to be generic and was shown to be equally effectively applicable to MCF-7 cells (Figures S9 and 2A).

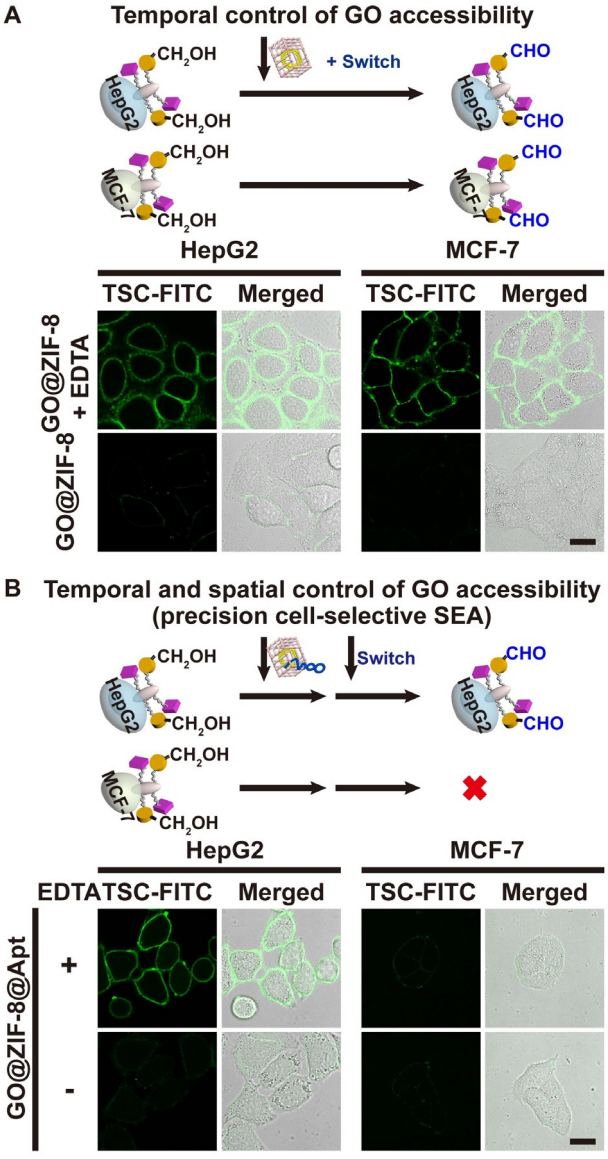

Figure 2. A) Temporal control and B) temporal, spatial control of GO accessibility for non-cell-selective (A) and cell-selective (B) surface terminal Gal/GalNAc remodeling. A) CLSM images of HepG2 and MCF-7 cells after treatment with GO@ZIF-8 or GO@ZIF-8/EDTA mixture and bioorthogonal labeling. B) CLSM images of HepG2 and MCF-7 cells after treatment with GO@ZIF-8@Apt, EDTA, and bioorthogonal labeling. Scale bars: 20 μm.

The refinement of the temporally controlled scheme further into both temporally and spatially controlled (cell-selective) SEA scheme required the participation of an additional component—a cell-targeting aptamer. An aptamer with high affinity for HepG2 cells, TLS11a (abbreviated as Apt), was therefore incorporated into the scheme.[14] The noncovalent conjugation of Apt to GO@ZIF-8 furnished GO@ZIF-8@Apt as the product, as evidenced by the shift of the zeta potential from positive to the negative regime (Figure S10). The cell viability remained high when incubated in GO@ZIF-8@Apt, ensuring its suitability for use in cell-related operation (Figure S9). The HepG2 cell-targeting capability of Apt was confirmed with the observation of lighting up of cell periphery when a 5′-Texas Red (TR)-conjugated Apt probe was used for GO@ZIF-8@Apt (Figure S11). The average number of GO@ZIF-8@Apt bound to each HepG2 cell was determined to be approximately 293. The cell recognition specificity of Apt was validated with MCF-7 cells as the negative control (Figure S11). Further quantification of cell periphery TR fluorescence intensity showed an Apt binding selectivity of 7.14:1 (from Apt) and 7.05:1 (from GO@ZIF-8@Apt) for HepG2 and MCF-7 cells.

With GO@ZIF-8@Apt as a readily deployed spatial and temporal control probe, the SEA-based cell-selective surface glycan remodeling was performed. The targeting of HepG2 with GO@ZIF-8@Apt did not lead to apparent transformation of terminal Gal/GalNAc (Figure 2B). Upon the engagement of 0.5 M EDTA, terminal Gal/GalNAc remodeling occurred instantaneously (Figure 2B). The execution of the whole SEA protocol required only 30 or even 24 min (15 min of cell targeting plus 15 or 9 min of glycan remodeling) (Figures S12 and 2B), which is much shorter than the approximately 72 h metabolic pathway approach.[6b] For further biocompatibility consideration, the concentration of EDTA could be reduced to 0.2 M (20 min of glycan remodeling) (Figure S13). The comparable cell periphery fluorescence intensity generated by SEA protocol and pristine GO (91.8%) (Figures 2B and S14) signifies highly efficient remodeling of accessible terminal Gal/GalNAc. The terminal Gal/GalNAc remodeling specificity was confirmed by the ability to competitively inhibit GO activity in the SEA protocol with solution-phase Gal (Figure S15). The contribution of each probe component was delineated by performing an otherwise identical SEA protocol except with the omission of the component of interest (Figure S14). The negligible cell periphery fluorescence intensity with the incubation of HepG2 cells in either ZIF-8@Apt or GO@ZIF-8, with or without further EDTA treatment, advocates the essential role played by both GO and Apt. ZIF-8 was also crucial because without this layer of SEA control, the GO portion of GO-Apt will be constitutively active toward non-cell-selective surface glycan remodeling. The SEA protocol was discriminatory against virtually all other cell lines lacking Apt affinity such as MCF-7 cells (Figures 2B and S14), thus allowing cell selectivity to be achieved (terminal Gal/GalNAc remodeling selectivity of 7.03:1 observed for HepG2 and MCF-7 cells, as dictated by Apt binding selectivity). With cell selectivity individually demonstrated, we then proceed to the more challenging task in this field: differentiation of different cell lines in close proximity in a co-cultured setting. The HepG2 and MCF-7 cells were co-cultured for 12 h in 1:1 seeding ratio and then subjected to treatment with the SEA protocol. 5′-TR conjugation to Apt allowed the identification of HepG2 cells and enabled fluorescence co-localization analysis to be performed. The SEA scheme proved to be a highly effective tool capable of providing superb spatial resolution (Figure 3): terminal Gal/GalNAc remodeling was exquisitely accomplished virtually exclusively on HepG2 cells, with the extent of remodeling positively correlated to the concentration of EDTA (Figures S16 and S17), whereas MCF-7 cells in the immediate neighbor were only minimally perturbed at the background level. The slightly lowered terminal Gal/GalNAc remodeling selectivity (6.08:1 for HepG2 and MCF-7 cells) likely reflects slightly compromised Apt binding selectivity in the complex cellular environment of co-cultured setting. Again, the constitutive catalytic activity of GO-Apt resulted in nondiscriminatory glycan remodeling for both HepG2 and MCF-7 cells (Figure 3). Each probe component was verified to be indispensable for the fulfillment of the SEA task (Figure S18).

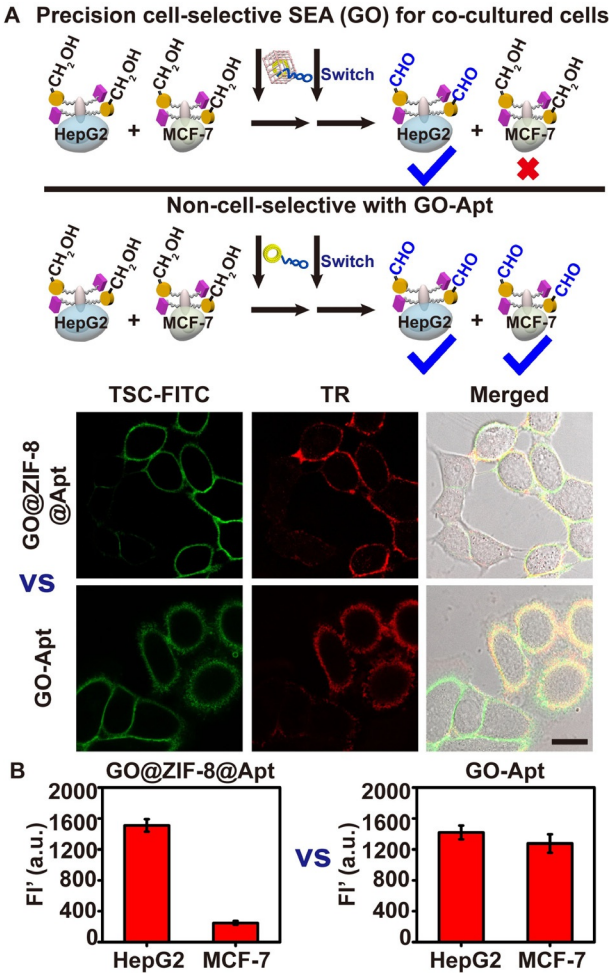

Figure 3. Precision cell-selective surface terminal Gal/GalNAc remodeling for co-cultured cells in close spatial proximity. A) CLSM images of co-cultured HepG2 and MCF-7 cells after initial treatment with GO@ZIF-8@Apt (5′-TR) and EDTA or GO-Apt (3′-TR), and subsequent bioorthogonal labeling. Scale bar: 20 μm. B) TSC-FITC fluorescence intensity (FI′) at the periphery of HepG2 and MCF-7 cells from (A) (from twenty different cells). $FI' = FI - FI_0$; FI_0: when GO@ZIF-8@Apt or GO-Apt concentration is zero.

To demonstrate the general applicability of the SEA scheme, a second enzyme, terminal sialic acid (Sia) cleavage enzyme α2-3,6,8,9-neuraminidase A (Neu),[15] was examined. The terminal Sia moiety was selected by virtue of its close association with tumor initiation and tumor progression.[2b] The temporally controlled switching of Neu from the inaccessible state in Neu@ZIF-8 to the accessible state could be triggered by EDTA (Figures S19, S20, and S21), leading to efficient desialylation on both HepG2 and MCF-7 cells and therefore diminished cell periphery fluorescence intensity, as probed with Sia-binding, fluorescent FITC-labeled Sambucus nigra agglutinin lectin (SNA-FITC). The fabrication of Neu@ZIF-8@Apt probe and implementation of the SEA protocol allowed selective desialylation only on HepG2 cells and not on MCF-7 cells (Figure S22). The ability to enforce accurate desialylation in the co-cultured setting of HepG2 and MCF-7 cells (Figures 4 and S23) testifies to the flexible modular adaptability as well as, again, to the high spatial resolving power of the SEA scheme.

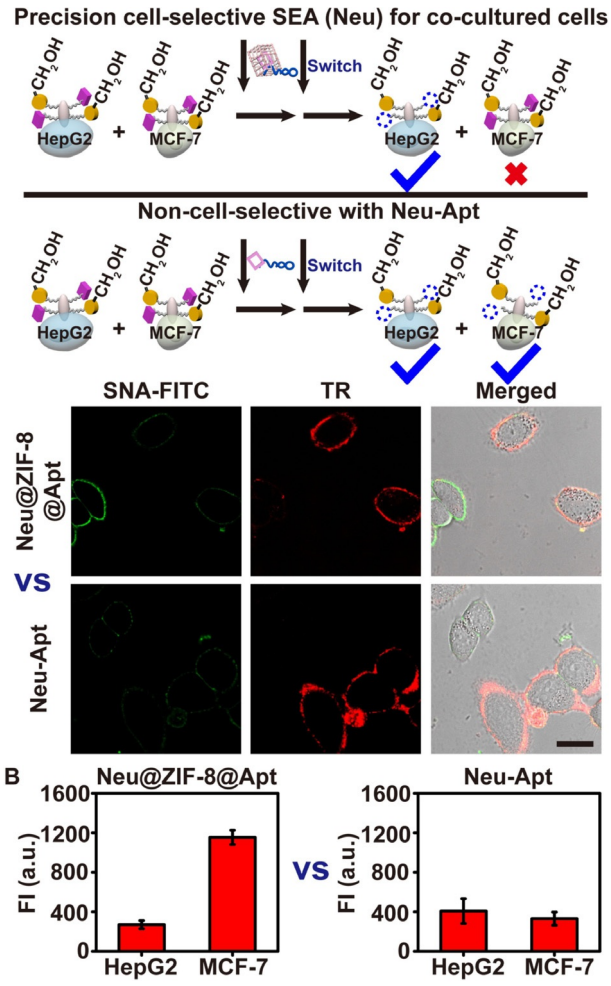

Figure 4. Precision cell-selective surface terminal Sia desialylation for co-cultured cells in close spatial proximity. A) CLSM images of co-cultured HepG2 and MCF-7 cells after initial treatment with Neu@ZIF-8@Apt (5′-TR) and EDTA or Neu-Apt (3′-TR), and subsequent SNA-FITC staining. Scale bar: 20 μm. B) SNA-FITC fluorescence intensity (FI) at the periphery of HepG2 and MCF-7 cells from (A) (from twenty different cells).

Conclusion

We have introduced herein the concept of SEA for cell-selective surface glycan remodeling. The stringent control of enzymatic accessibility at the cell-targeting delivery stage and on-cell glycan remodeling stage has enabled the previously existing constitutive enzymatic activity issue to be fully solved. With its modular design, the SEA scheme is expected to be capable of serving as a general cell-selective precision remodeling tool for surface-confined structures and, as such, should contribute tremendously to the understanding of cell-surface dynamics, modulation of cell-surface functions, and theranostics of diseased states.

Experimental Section

Synthesis of GO@ZIF-8: A biomimetic mineralization method was used for the preparation of GO@ZIF-8.[8,12] In particular, an aqueous solution containing GO (4 mg mL^{-1}, 0.04 mL) and 2-MIM (1 M, 0.4 mL) was mixed with an aqueous solution of $Zn(NO_3)_2{\cdot}6H_2O$ (0.15 M, 0.04 mL) at RT (r.t.). The solution turned from transparent to opaque within 1 min, suggesting the formation of crystals. After reaction for 30 min under stirring, the product was collected by centrifugation at 10,000 rpm for 10 min and three times washing with water, and then re-suspended in water. The adsorbed GO on the outside surface of as-prepared GO@ZIF-8 was removed by dispersing GO@ZIF-8 in 1 mL of 5% PVP solution, stirring for 10 min, and centrifugation to discard the supernatant. This PVP exchange procedure was repeated for two more times. The product was washed three times with 1 mL of PBS to fully remove excess PVP.

In vitro analysis of GO and GO@ZIF-8 activity using Amplex® Red Gal/GO Kit: After mixing of 5 μL PBS solution containing GO or GO@ZIF-8 (0.05 mg mL^{-1} in GO unit), in the presence or absence of EDTA, with 45 μL 1×Reaction Buffer (0.05 M Tris-HCl, pH 7.2, 1 mM $CaCl_2$), a PBS solution (50 μL) containing 100 μM Amplex Red Reagent, 0.2 U mL^{-1} HRP, and 200 μM Gal was added. The reaction was allowed to proceed at 37 °C for 1 h, and then the emission signal at ca. 590 nm (excitation wavelength: 540 nm) was measured.

Monitoring of GO and GO@ZIF-8 activity: A 50 μL Reaction Buffer containing 200 mU mL^{-1} GO or GO@ZIF-8 (determined by Amplex® Red Gal/GO Kit as mentioned above) was added to a 50 μL Reaction Buffer containing 100 μM Amplex Red Reagent, 0.2 U mL^{-1} HRP, and 200 μM Gal or 100 μM Lac (or replaced by 250 μg mL^{-1} MUC2, 300 μg mL^{-1} fixedly suspending HepG2 cells or MCF-7 cells and 2 U mL^{-1} GO or GO@ZIF-8, respectively). The reaction was allowed to proceed at 37 °C for 1 h, and then the emission signal at ca. 590 nm (excitation wavelength: 540 nm) was measured. Note: The fixedly suspending cells were prepared as follows. First, the cells were digested by trypsin; then, after three times washing with PBS (1,000 rpm, 5 min), the cells were dispersed overnight at 4 °C in 70% cold ethanol.

Demonstration of the removal of surface-trapped GO for GO@ZIF-8 by PVP treatment: The HepG2 cells were seeded and blocked, then respectively incubated with GO@ZIF-8 (without PVP treatment), GO@ZIF-8 (with PVP treatment), and GO (0.05 mg mL^{-1} in GO unit) at 4 °C for 15 min, respectively. After three times washing with PBS and bioorthogonal labeling, the cells were immediately imaged with CLSM. The emission signal from 505 to 565 nm was collected with CLSM under 495 nm excitation.

Verification of GO caging and EDTA-triggered uncaging: The cells (HepG2 or MCF-7) were seeded and blocked as described above, and then subjected to incubation with a mixture of GO@ZIF-8 and 0.5 M EDTA, GO@ZIF-8, or GO (0.05 mg mL^{-1} in GO unit) in 100 μL PBS at 4 °C for 15 min, respectively. After three times of washing with PBS and bioorthogonal labeling, the cells were immediately imaged with CLSM.

Apt conjugation to GO@ZIF-8 (GO@ZIF-8@Apt): PBS buffer (8 μL) containing 2 μM Apt was mixed with 0.4 mL, 0.05 mg mL^{-1} GO@ZIF-8 solution. The mixture was further gently shaken at r.t. for 2 h, followed by centrifugation at 10,000 rpm for 10 min and three times washing with PBS buffer. The product was then stored at 4 °C (shielded from light).

Demonstration with CLSM of GO@ZIF-8@Apt-based cell-selective Gal/GalNAc remodeling: After seeding and blocking, HepG2 (or MCF-7) cells were incubated with GO@ZIF-8@Apt, GO@ZIF-8, ZIF-8@Apt, GO-Apt, and GO (0.05 mg mL^{-1} in GO unit), respectively, at 4 °C for 15 min, followed by three times washing with PBS. Then for the former three types of probes, half of the corresponding wells were treated with 0.5 M EDTA at 4 °C for 15 min. As a control, during this step, the other wells without EDTA treatment were left in 100 μL of PBS buffer. After PBS washing and bioorthogonal labeling, the cells in all the wells were observed with CLSM with emission range set from 505 to 565 nm under 495 nm excitation.

Precision cell-selective Gal/GalNAc remodeling in co-cultured setting: HepG2 and MCF-7 cells were each seeded at a density of 5×10^5 cells mL^{-1}, and co-cultured in DMEM medium for 12 h. After blocking and washing steps, the co-cultured cells were then incubated with 0.05 mg mL^{-1} GO@ZIF-8@TR-Apt, GO@ZIF-8, ZIF-8@TR-Apt, GO-Apt-TR, and GO (all in GO unit) at 4 °C for 15 min, respectively. Following PBS washing, the cells were incubated with EDTA at 4 °C for 15 min. After washing, bioorthogonal labeling was performed on cells. The cells were further co-stained with TR-Apt at 4 °C for 15 min for co-localization (except the wells containing GO@ZIF-8@TR-Apt, ZIF-8@TR-Apt, GO-Apt-TR). The cells were then carefully washed and imaged with CLSM. The emission signals were collected from 505 to 565 nm and from 605 to 685 nm with CLSM under 495 nm and 594 nm excitation, respectively.

Acknowledgements

We gratefully acknowledge support from the National Natural Science Foundation of China (21675082), the National Key Research and Development Program of China (2018YFC1004704), Fundamental Research Funds for the Central Universities (020514380184), and State Key Laboratory of Analytical Chemistry for Life Science (5431ZZXM1903).

Conflict of interest

The authors declare no conflict of interest.

Keywords: carbohydrates · cell recognition · glycan remodeling · imaging agents · metal–organic frameworks

[1] L. Morsut, K. T. Roybal, X. Xiong, R. M. Gordley, S. M. Coyle, M. Thomson, W. A. Lim, *Cell* **2016**, *164*, 780 – 791.
[2] a) A. Varki, *Glycobiology* **2017**, *27*, 3 – 49; b) S. S. Pinho, C. A. Reis, *Nat. Rev. Cancer* **2015**, *15*, 540 – 555.
[3] J. E. Hudak, S. M. Canham, C. R. Bertozzi, *Nat. Chem. Biol.* **2014**, *10*, 69 – 75.
[4] a) J. A. Prescher, D. H. Dube, C. R. Bertozzi, *Nature* **2004**, *430*, 870 – 873; b) S. H. Rouhanifard, L. U. Nordstrom, T. Zheng, P. Wu, *Chem. Soc. Rev.* **2013**, *42*, 4284 – 4296; c) Y. Chen, L. Ding, H. Ju, *Acc. Chem. Res.* **2018**, *51*, 890 – 899.
[5] a) H. Xiao, E. C. Woods, P. Vukojicic, C. R. Bertozzi, *Proc. Natl. Acad. Sci. USA* **2016**, *113*, 10304 – 10309; b) E. Rodríguez, S. T. Schetters, Y. van Kooyk, *Nat. Rev. Immunol.* **2018**, *18*, 204.
[6] a) Y. Sun, S. Hong, R. Xie, R. Huang, R. Lei, B. Cheng, D. Sun, Y. Du, C. M. Nycholat, J. C. Paulson, X. Chen, *J. Am. Chem. Soc.* **2018**, *140*, 3592 – 3602; b) M. K. Shim, H. Y. Yoon, J. H. Ryu, H. Koo, S. Lee, J. H. Park, J. H. Kim, S. Lee, M. G. Pomper, I. C. Kwon, K. Kim, *Angew. Chem. Int. Ed.* **2016**, *55*, 14698 – 14703; *Angew. Chem.* **2016**, *128*, 14918 – 14923.
[7] a) H. Li, J.-M. Hah, D. S. Lawrence, *J. Am. Chem. Soc.* **2008**, *130*, 10474 – 10475; b) M. Ghosh, X. Song, G. Mouneimne, M. Sidani, D. S. Lawrence, J. S. Condeelis, *Science* **2004**, *304*, 743 – 746.
[8] a) K. Liang, R. Ricco, C. M. Doherty, M. J. Styles, S. Bell, N. Kirby, S. Mudie, D. Haylock, A. J. Hill, C. J. Doonan, P. Falcaro, *Nat. Commun.* **2015**, *6*, 7240; b) K. Liang, J. J. Richardson, C. J. Doonan, X. Mulet, Y. Ju, J. Cui, F. Caruso, P. Falcaro, *Angew. Chem. Int. Ed.* **2017**, *56*, 8510 – 8515; *Angew. Chem.* **2017**, *129*, 8630 – 8635; c) C. Doonan, R. Riccò, K. Liang, D. Bradshaw, P. Falcaro, *Acc. Chem. Res.* **2017**, *50*, 1423 – 1432; d) K. Liang, J. J. Richardson, J. Cui, F. Caruso, C. J. Doonan, P. Falcaro, *Adv. Mater.* **2016**, *28*, 7910 – 7914; e) K. Liang, C. Carbonell, M. J. Styles, R. Ricco, J. Cui, J. J. Richardson, D. Maspoch, F. Caruso, P. Falcaro, *Adv. Mater.* **2015**, *27*, 7293 – 7298; f) W. Liang, R. Ricco, N. K. Maddigan, R. P. Dickinson, H. Xu, Q. Li, C. J. Sumby, S. G. Bell, P. Falcaro, C. J. Doonan, *Chem. Mater.* **2018**, *30*, 1069 – 1077; g) W. Liang, H. Xu, F. Carraro, N. K. Maddigan, Q. Li, S. G. Bell, D. M. Huang, A. Tarzia, M. B. Solomon, H. Amenitsch, L. Vaccari, C. J. Sumby, P. Falcaro, C. J. Doonan, *J. Am. Chem. Soc.* **2019**, *141*, 2348 – 2355.
[9] a) C. Brieke, F. Rohrbach, A. Gottschalk, G. Mayer, A. Heckel, *Angew. Chem. Int. Ed.* **2012**, *51*, 8446 – 8476; *Angew. Chem.* **2012**, *124*, 8572 – 8604; b) G. C. R. Ellis-Davies, *Nat. Methods* **2007**, *4*, 619.
[10] Q. Wang, X. Zhang, L. Huang, Z. Zhang, S. Dong, *Angew. Chem. Int. Ed.* **2017**, *56*, 16082 – 16085; *Angew. Chem.* **2017**, *129*, 16298 – 16301.
[11] K. K. Palaniappan, C. R. Bertozzi, *Chem. Rev.* **2016**, *116*, 14277 – 14306.
[12] a) J. Cui, Y. Feng, T. Lin, Z. Tan, C. Zhong, S. Jia, *ACS Appl. Mater. Interfaces* **2017**, *9*, 10587 – 10594; b) J. Zhuang, C.-H. Kuo, L.-Y. Chou, D.-Y. Liu, E. Weerapana, C.-K. Tsung, *ACS Nano* **2014**, *8*, 2812 – 2819.
[13] S. R. Stowell, T. Ju, R. D. Cummings, *Annu. Rev. Pathol. Mech. Dis.* **2015**, *10*, 473 – 510.
[14] L. Kashefi-Kheyrabadi, M. A. Mehrgardi, E. Wiechec, A. P. Turner, A. Tiwari, *Anal. Chem.* **2014**, *86*, 4956 – 4960.
[15] Y. Li, X. Chen, *Appl. Microbiol. Biotechnol.* **2012**, *94*, 887 – 905.

Manuscript received: May 8, 2019
Revised manuscript received: June 4, 2019
Accepted manuscript online: June 7, 2019
Version of record online: July 8, 2019